Curie-temperature enhancement of electron-doped Sr_2FeMoO_6 perovskites studied by photoemission spectroscopy

J. Navarro and J. Fontcuberta
Institut de Ciència de Materials de Barcelona Campus U.A.B., Bellaterra 08193, Catalunya, Spain

M. Izquierdo, J. Avila, and M. C. Asensio
LURE, Centre Universitaire Paris-Sud, Bât. 209D, B.P. 34, 91405 Orsay Cedex, France
and Instituto de Ciencia de Materiales, CSIC, 28049 Madrid, Spain

(Received 19 March 2003; revised manuscript received 30 May 2003; published 3 March 2004)

We report here on the electronic structure of electron-doped half-metallic ferromagnetic perovskites such as $Sr_{2-x}La_xFeMoO_6$ ($x=0-0.6$) as obtained from high-resolved valence-band photoemission spectroscopy (PES). By comparing the PES spectra with band-structure calculations, a distinctive peak at the Fermi level E_F with predominantly (Fe+Mo) $t_{2g}^{\downarrow}$ character has been evidenced for all samples, irrespectively of the x values investigated. Moreover, we show that the electron doping due to the La substitution provides selectively delocalized carriers to the $t_{2g}^{\downarrow}$ metallic spin channel. Consequently, a gradual rising of the density of states at the E_F has been observed as a function of the La doping. By changing the incoming photon energy we have shown that electron doping mainly rises preferentially the Mo density of states. These findings provide fundamental clues for understanding the origin of ferromagnetism in these oxides and shall be of relevance for tailoring oxides having still higher T_C.

DOI: 10.1103/PhysRevB.69.115101 PACS number(s): 79.60.−i, 71.45.Lr, 64.60.−i, 73.20.At

I. INTRODUCTION

The early discovery of colossal magnetoresistance has abundantly stimulated the research on manganese oxides because of their leading technological applications, not counting their critical importance in basic physics. However, typically the magnetoresistance strength diminishes as the Curie temperature (T_C) increases up to room temperature, thus making it difficult the direct technological use of these advanced materials. As progress of spintronics requires fully spin-polarized ferromagnetic materials, having T_C well above room temperature, the recent finding of room-temperature tunneling magnetoresistance and half-metallic (HM) behavior in Sr_2FeMoO_6 (SFMO) oxides with $T_C \sim 400$ K (Ref. 1) has opened renewed interest and expectations for promising applications. $A_2MM'O_6$ double perovskites are built up by alternate $M'O_6$ and MO_6 octahedral units bonded by oxygen bridges, where A is an alkaline earth or rare-earth ion and M, M′ are $3d$ and $4d/5d$ transition metals. These materials are predicted to be HM,[1–4] where the metallic behavior of one electron spin channel is coexisting with an energy gap between valence and conduction bands for the electrons of the other spin polarization. In short, the electronic configuration of SFMO can be described by $Fe(3d^{6-\delta})$:$Mo(4d^{\delta})$ ($\delta=0.3$[5]). The Fe-$3d$ fullfilled (t_{2g}^3 and e_g^2) spin-up electrons can be viewed as localized whereas the Fe $3d$ partially empty ($t_{2g}^{1-\delta}$) spin-down states are strongly hybridized with O-$2p$ orbitals and partially empty Mo-$4d^{\delta}$ (spin-down) states. Consequently, these transition-metal oxides alloys present bands associated to one spin polarization (in this case Fe-$3d$ spin-up) entirely filled, and separated by an energy gap from the other spin channel involving Fe-$3d$ and Mo-$4d$ spin-down electrons has a metallic character.

Recent photoemission spectroscopy (PES) experiments[6–8] have provided evidence of the half-metallic character of SFMO by determining that the states close to the Fermi level have predominantly Mo $t_{2g}^{\downarrow}$ and Fe $t_{2g}^{\downarrow}$ character: by comparing the measured valence-band spectra with the local spin-density approximation (LSDA) band-structure theoretical calculations it has been concluded that the delocalized electrons at the E_F are totally spin-down polarized. Consistent results have been lately obtained by using x-ray absorption spectroscopy experiments.[9] The site-specific reported information is also in agreement with LSDA theoretical calculations which contemplate that well localized t_{2g}^3 and e_g^2 spin-up Fe-$3d$ subbands are well below the Fermi level and that the delocalized t_{2g} spin-down subbands due to the Mo($4d$) and Fe ($3d$) are at the E_F. These spectroscopic results together with recent magnetic measurements in the paramagnetic phase[10] support that the AFM interaction is driven by a mechanism where the itinerant carriers and the Fe localized cores tend to be antiparallel, at variance with the double exchange interaction.

Magnetic measurements are consistent with ferromagnetic ordering of $Fe(3d^{6-\delta})$ moments which shall be antiferromagnetically coupled to any moment on $Mo(4d^{\delta})$ sites. Understanding of the physical mechanism lying behind the ferromagnetic ordering remains challenging. Difficulties arise mainly due to the fact that in this structure the $4d$(Mo) ions are essentially nonmagnetic and thus the separation between the magnetic ions [$3d$(Fe)] is substantially large (~ 8 Å). In spite of this, the Curie temperature is very high, exceeding that of the celebrated manganites ($T_C < 360$ K). This observation suggests that the double exchange model used to describe the ferromagnetism in manganites cannot be safely used in the present case. Sarma *et al.*[6] proposed that due to the Fe-Mo hybridization, the intra-atomic exchange in Mo is

much enhanced thus resulting in a strong antiferromagnetic coupling between Fe and Mo and thus leading to an effective more robust Fe-Fe ferromagnetic ordering. Recently, Fang *et al.*[11] have proposed that ferromagnetism is stabilized by the exchange splitting of the Mo($4d$) orbitals, which lowers the energy of carriers and promotes a charge transfer from the spin-up to the spin-down subbands.

Based on neutron diffraction[1,12,13] and early Mössbauer spectroscopy data,[14] ferrimagnetism was proposed to be originated from the AFM ordering of Fe^{3+} ($3d^5$; $t_{2g}^{3\uparrow}\ e_g^{2\uparrow}$): Mo^{5+}($4d^1$; $t_{2g}^{1\downarrow}$) configurations, thus predicting a saturation magnetization of $4\mu_B$. However, the experimental values of the saturation moment are commonly found to be of about 3.1-3.2μ_B.[1,14–16] So far, this sensible diminution of the saturation moment has been attributed to a partial Fe-Mo disorder. From more recent Mössbauer data, however, a state of valence fluctuation of $Fe^{2.5+}$ has been proposed by Lindén *et al.*[17] and Balcells *et al.*,[5] and this has been sustained by Chmaissen *et al.* who has found $\mu_{Fe}=(4.3–4.4)\mu_B$ from neutron diffraction and Mössbauer studies.[18] We recall that, as indicated in reference 5, the saturation magnetization values can not allow discriminating among Fe^{3+}:Mo^{5+} or Fe^{2+}:Mo^{6+} electronic configurations. In contrast, the effective moment in the paramagnetic phase shall be insensitive to the presence of Fe/Mo disorder and should, in principle, allows to discriminate between Fe^{3+}:Mo^{5+} or Fe^{2+}:Mo^{6+} configurations, thus it may provide a more robust insight into the electronic configuration of the Fe/Mo ionic species. Using this approach, Tovar *et al.* have recently shown that the magnetic properties in the paramagnetic regime cannot be understood by considering only the contribution of localized moments: the effective paramagnetic moment is found to be smaller that it should be expected for any electronic configuration Fe($3d^6$):Mo($4d^0$) or Fe($3d^5$):Mo($4d^1$).[19]

In fact, the paramagnetic susceptibility data has been modeled[10] by assuming that there is an exchange induced spin polarization of the conduction band being antiferromagnetically coupled to the localized moments by Hund coupling. Even more, the strength of the ferromagnetic coupling has been predicted to be proportional to the density of states at the Fermi level [$D(E_F)$]. These findings may provide microscopic understanding of the observed augmentation of the Curie temperature upon electron doping[20] although direct evidence is still lacking. Similarly, evidence of a half-metallic ferromagnetic nature of these electron-doped double perovskites is still missing.

Here, we report on synchrotron radiation photoemission measurements near the Fermi level of $Sr_{2-x}La_xFeMoO_6$ with a gradual level of electron doping. As it has been recently shown,[20] the doping (achieved via partial substitution of Sr^{+2} by La^{+3}) promotes a substantial enhancement of the Curie temperature (with ΔT_C up to 80 K). These experimental evidences, sharply contrast with some recent predictions[21] thus illustrating the complexity of phase diagram in double perovskites. We will show here that as the La substitution progresses, a noticeable enhancement of the $D(E_F)$ mainly formed by Mo($4d$) and Fe ($3d$) states is measured. A clear correlation between $D(E_F)$ and T_C is discovered. In addition, we provide spectroscopic evidence that the electron injection supplies carriers to the metallic spin-down channel; while the other Fe-$3d$ fullfilled (t_{2g}^3 and e_g^2) spin-up insulating channel remains unchanged. These results constitute a stringent test for proposed models for electronic structure and ferromagnetism in SFMO and shall provide guidelines for further progress on tailoring ferromagnetic metals having optimal properties for spintronics.

II. EXPERIMENTAL DETAILS

PES experiments on $Sr_{2-x}La_xFeMoO_6$ ceramic samples have been performed at the ANTARES (SU8 beamline) at LURE using synchrotron radiation light between 14 and 890 eV provided by an insertion device of Super-Aco storage ring.[22,23] The Fermi level of the oxides has been determined using Cu as reference. In the range of explored energies hν the energy resolution has been of about 50–150 meV.[23–25] The spectra intensity has been normalized with respect to the source photon flux, which has been measured using the photoinduced current I_0 of a gold grid placed behind the sample. In order to take into account a constant detection geometry and the optimal analyzer focus for all samples analyzed, we have considered a spectral feature sensible to these parameters. As it is known in PES experiments, the absolute value of the background intensity in the flat zones of the spectra is particularly affected by the above-mentioned experimental parameters. Consequently, the quantitative evaluation presented in this work has been done considering the absolute background intensity value at 5 eV above the Fermi level. Only those samples, whose background intensity is comparable (within 2% of error) have been considered. Moreover, any particular alignment has been imposed, nor any additional normalization procedure has been taken into account.

Due to the polycrystalline nature of the investigated samples, the results reported here should be considered as angle-integrated data, because the lack of momentum discrimination in the reciprocal space. Samples have been scratched in situ in ultrahigh vacuum ($P<3\times10^{-11}$ torr) by using a diamond saw. Surface contamination has been monitored by synchrotron radiation photoemission. All investigated samples showed a very high level of reactivity. Minor photoemission features near the Fermi level were much more affected by small amount of carbon and/or oxygen contamination than strong PES features at high binding energies. The correct cleanliness of the samples was achieved ensuring excellent UHV conditions and the confirmation that any trace of contamination were present in them. All measurements have been carried out at room temperature.

Sample preparation, structural and magnetic characterization can be found elsewhere.[5,19,20] Here, in order to illustrate the high quality of the used samples, we only mention that in the pristine compound ($x=0$), the saturation magnetization is $M_S=3.8\mu_B$ and the antisite concentration (i.e., misplaced Fe/Mo ions) is $\sim5\%$ and the Curie temperature (determined from extrapolation of the magnetization curves) is of about 430 K. For the rest of samples the corresponding values are

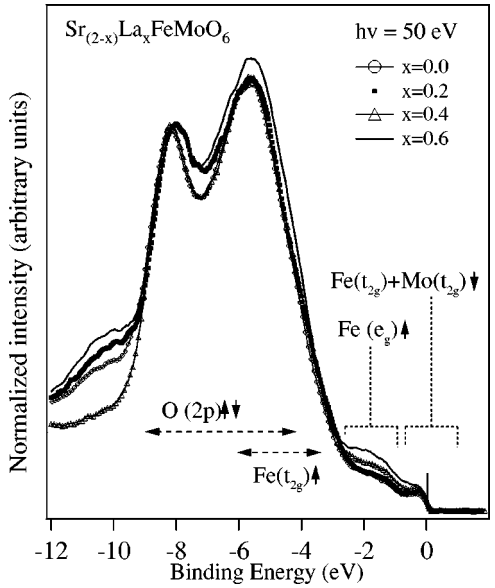

FIG. 1. Valence-band spectra photoemission spectra for $Sr_{2-x}La_xFeMoO_6$ ($x=0-0.6$) recorded at $h\nu=50$ eV. In the bottom part, theoretical calculations adapted from Ref. 1 are included.

$T_C=440$ K, 465 K, and 480 K for $x=0.2$, 0.4, and 0.6, respectively. These T_C values are comparable to those reported in Ref. 20 for similar samples. The T_C values determined from the Arrot plots also show the same systematic rise with doping although the absolute values are somewhat lower; for instance $T_C=400$ K and 420 K for $x=0$ and 0.4, respectively. Refinement of neutron-diffraction profiles have been used to confirm that, within the experimental resolution, all samples reported here have oxygen stoichiometric content.[26]

III. RESULTS

Figure 1 shows the valence-band spectrum of $Sr_{2-x}La_xFeMoO_6$ ($x=0$, 0.2, 0.4, and 0.6) samples collected using $h\nu=50$ eV. The same spectra have been measured using a wide photon energy range (not shown), including near $h\nu=90$ eV where Mo states present a Cooper minimum and thus the PES is mainly dominated by Fe($3d$) and O($2p$) states. The significant photoemission features of the valence band of these compounds are present in all spectra measured in the 30 eV$<h\nu<$170 eV photon energy range. It is noticeable, that the relative intensity of the peaks in each spectra depends on the photon energy used due to the well-known energy dependence of the matrix elements. These results are in excellent agreement with recent published data for SFMO (Ref. 8) and Ba_2FeMoO_6 (Ref. 7) double perovskites.

As we will show below, all significant valence-band photoemission features recorded from the La-doped SFMO samples closely correspond to those for the parent compound valence band. In the past, the assignation of every peak has been basically done comparing experimental valence-band spectra with theoretical density of states calculations.[1,7,8] In order to correlate the measured La-doped samples spectral weight with the dominating integrated density of states of these compounds, we included in the bottom of the Fig. 2, the first reported theoretical density of states for the SFMO, from Kobayashi *et al.*[1] These results, based on the generalized gradient approximation for the exchange and correlation part of the density-functional method, give the spin discriminated bands characteristic of SFMO. Subsequently, several theoretical groups have performed band-structure calculations for the SFMO. In particular, Wu *et al.*[4] and Saitoh *et al.*,[8] by using full-potential linearized augmented plan-wave method within the LSDA and LSDA+U scheme, have showed that the generic features of the SFMO valence band are consistent with the GGA calculations.[1] The only noticeable change induced by the introduction of an effective Coulomb repulsion U_{eff}, concerns the binding energy of the spin-up Fe(t_2g) states, which are shifted down in energy.[8,4,7]

Regarding Fig. 1, it can be noticed that two major features, occurring at -8 and -6 eV correspond to O($2p$) and Fe($e^{\uparrow}_{t2g}$) states, respectively, as it has been reported before for nonelectron doped samples.[7,8] Experimentally, the metallic edge is clearly visible for all samples. In addition well-defined features are observed at binding energies (BE) extended from ~-2.5 eV to ~-10 eV, below the Fermi level. In agreement with computations,[1,4,9] the experimental peaks can be safely assigned to two dominating features, one mainly spin-up and spin-down O($2p$)-hybridized band extended from -9 eV to -2 eV and one sharp large peak near the upper band edge associated to the spin-up Fe($t2g$) states, which extends from -6 eV to -2 eV. The metallic edge can be well recognized for all x values. At the bottom of the valence band, we observe a broad feature at 9–12 eV. This peak has not been reported in La-nondoped samples, hence it has not been so far assigned. It cannot be associated to any contamination because the cleanliness of the samples was carefully and regularly checked by synchrotron radiation photoemission. Alternatively, even if theoretical band-structure calculations of La-doped compounds are not available, we may speculatively relate this peak to Fe-O hybridized states, which could be associated to the existence of a structural phase transition in these samples. At $x=0.6$ this phase transition is well established, however, at lower doping values, it is supposed to be present but only partially, in a way, which is rather difficult to ascertain quantitatively.

Substantial modifications of the spectra are observed at or around (0–2 eV) the Fermi level upon La substitution. Within the context of this paper of the greatest interest is the valence-band spectrum close to the E_F as shown in Fig. 2. To elucidate the origin of the observed changes in the spectra, we have recorded spectra at different photon energies with the purpose of taking advantage of the dependence of the photoionization cross sections σ of the different elements on the photon energy. Detailed inspection of these spectra immediately reveals a finer structure. At $h\nu=90$ eV [Fig. 2 (top)], where the cross section of the Fe electronic states is much higher than those from molybdenum and oxygen [σ(Fe):σ(Mo):σ(O)$\sim$7:0.1:1.5], the spectra show two main features, one state at the Fermi edge which changes slightly its intensity as the electron doping progresses and other state extended from 0.7 eV to 2.5 eV, whose intensity is

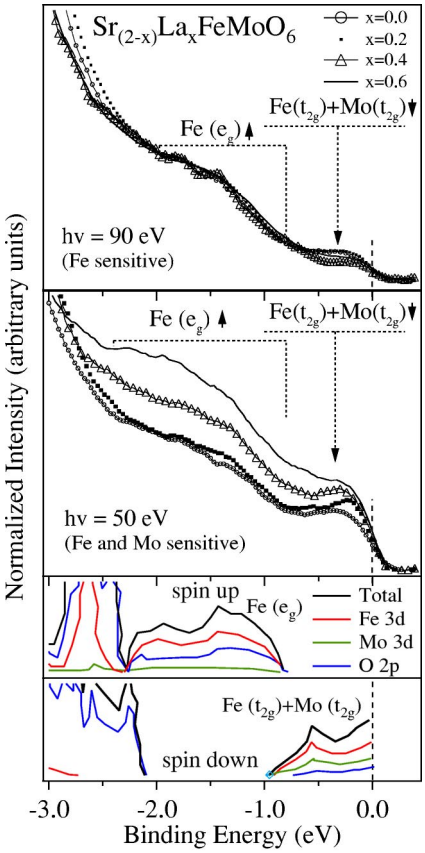

FIG. 2. (Color online) Photoemission spectra near E_F region of $Sr_{2-x}La_xFeMoO_6$ ($x=0-0.6$) recorded at $h\nu=90$ eV (top) and $h\nu=50$ eV (middle). In the bottom part, theoretical calculations adapted from Ref. 29 are included.

unchanged as the La doping increases.

In Fig. 2 (middle) we show the same spectra recorded at $h\nu=50$ eV, where the cross sections of Fe, Mo, and O ions are comparable [σ(Fe):σ(Mo):σ(O)$\sim$9:3.5:6]. Both features are present; however, their behavior as a function of doping is different: in this case, the intensity of both states is clearly rising as the La content increases, thus revealing a gradual modifications of Mo and O derived states. We include in Fig. 2 (bottom) the theoretical density of states for the parent compound as recently calculated by Saitoh *et al.*[8] In agreement with computations,[1,4,11,8] we note that the experimental features observed in the PES can be assigned to: oxygen O($2p$) hybridized spin-up Fe(e_g) ($-1--2.5$ eV) states and spin-down Fe(t_{2g})+Mo(t_{2g}) states (0 to -1 eV).

Deconvolution of the experimental data has been done (Fig. 3) using a background Gaussian function that collects the tail of the -6 eV peak (Fig. 2) plus three gaussian peaks, labeled *C*, *B*, and *A* convoluted with the Fermi function in Fig. 3. The solid line through the data shows the quality of the fits. This decomposition allows a clear identification of the states (B at ~-2.0 eV and C at ~-1.25 eV), corresponding to the spin-up Fe(e_g) doublet band predicted by several theoretical works.[1–4,6–8,11] The expected theoretical bandwidth of 1.5 eV for the spin-up Fe($e_g^{\uparrow}$) states agrees quite well with the states labeled as *B* and *C*. Taking into

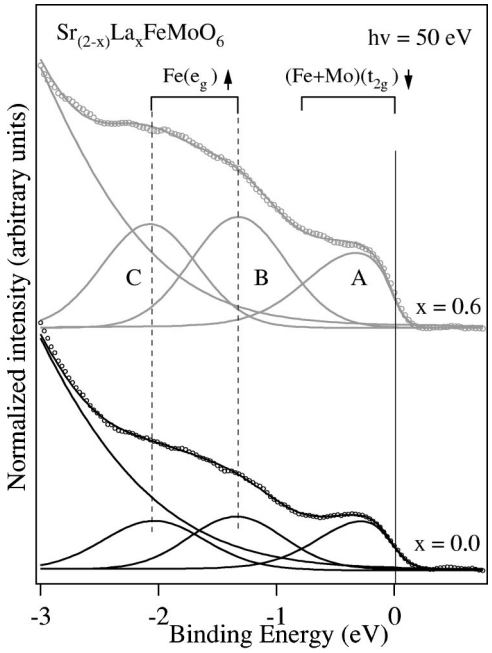

FIG. 3. Upper part of the valence-band spectra for $Sr_{2-x}La_xFeMoO_6$ ($x=0,0.6$), recorded at $h\nu=50$ eV. Deconvolution of different states are indicated.

account the spectral weight broadening due to the relative high measurement temperature, we can estimate the photoemission half-gap on the occupied state side of the majority spin-up Fe($e_g^{\uparrow}$) channel to be 0.7 ± 0.2 eV. The peak labeled A, extending up to the Fermi level, can be associated to spin-down Fe($t_{2g}^{\downarrow}$) and Mo($t_{2g}^{\downarrow}$) states. The comparison of the PES spectra with theoretical predictions[1,8] shown in Fig. 2 confirms the peak assignation we have made. From data in Fig. 2, it is clear that the position of the spin-up Fe($e_g^{\uparrow}$) states (*B* and *C*), does not change noticeably with La doping, indicating that the spin-up (majority) channel gap is not perturbed by the electron injection all along the investigated doping regime.

It is important to note that, in agreement with recent predictions,[21] the results shown in Fig. 3 indicate that a simple rigid-band model cannot be used to analyze the data. In this framework, it shall be expected that a charge transfer or carrier doping may promote a rigid upward shift of the Fermi level in order to fill with the extra charge *available unoccupied bands*. If this was the case the binding energy of both spin channels should have been increased in the same amount as the Fermi level may have been shifted. In spite of this, only the states at the Fermi level (feature *A* of Fig. 2) associated to the delocalized spin-down Mo states are modified. The spectral weight related to those totally polarized states increases and their binding energy shifts slightly away from the Fermi level. In contrast, features *B* and *C* associated to the spin-up channel are not affected by the electron doping keeping their binding energy unchanged for different La content. Consequently, the photoemission half-gap on the occupied state side of the minority spin-up Fe($e_g^{\uparrow}$) channel remains invariable ($<0.7\pm0.2$ eV) irrespectively on doping.

In order to evaluate the behavior of the intensity of peaks

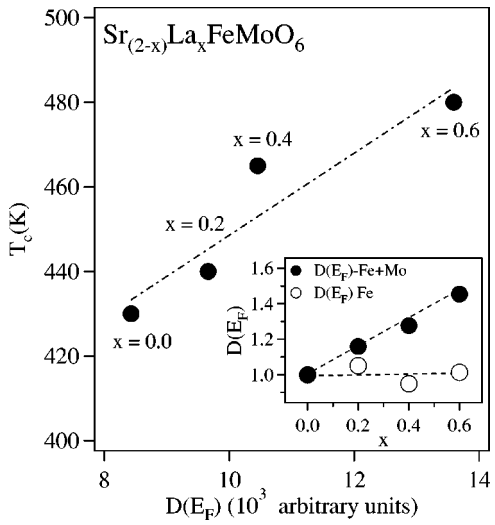

FIG. 4. Curie temperature vs the density of states $D(E_F,x)$ taken at 50 eV. Inset: Normalized $D(E_F)=D(E_F,x)/D(E_F,0))$ taken at 50 eV (●) and 90 eV (○) vs the La contents.

A, *B*, and *C*, we concentrate our analysis on the PES spectra (Fig. 2) obtained at the Mo Cooper minimum ($h\nu=90$ eV), with purpose to discriminate the relative contribution of the Fe and Mo to the corresponding states. Top part of Fig. 2 reveals that at $h\nu=90$ eV the $t_{2g}^{\downarrow}$ states do not change their intensity upon La doping, thus indicating that the enhancement observed at $h\nu=50$ eV is due to the some progressive admixture of Mo (*A*) and oxygen hybridized orbitals (*B* and *C*), to the bottom of the conduction and top of the valence band, respectively. Of fundamental importance is the observation that at $h\nu=50$ eV (and to lower extent also for $h\nu=90$ eV) the intensity of the $t_{2g}^{\downarrow}$ peak (labeled *A*) increases and thus the corresponding density of states at the Fermi level $D(E_F)$ also rises. This is a key result that reveals that La doping and the accompanying electron injection promote an enhancement of $D(E_F)$. The fact that this effect is almost canceled when photons insensitive to Mo states are used, suggests that the electron doping supplies charge almost exclusively to previously unoccupied spin down ↓ Mo states, although these states may be strongly hybridized with oxygen and Fe states. Moreover, independently of the photon energy used, the data undoubtedly show that the BE of the spin-up channel remains unaffected by the La electron doping, whereas the spin-down channel close to the Fermi level is affected both in BE and intensity.

The density of states $D(E_F)$ has been evaluated by integrating the measured PES intensity measured at 50 eV (Fe and Mo sensitive, Fig. 2 (middle) over an energy range of ± 100 meV around the Fermi-edge inflexion point. As shown in Fig. 4 (inset), where we collect the normalized $D(E_F)$ vs La concentration (x) (solid circles), there is a roughly linear enhancement of $D(E_F)$ upon doping. We have tested the robustness of this result by integrating the PES intensity over other energy ranges (50–200 meV). No significant variation of the $D(E_F,x)$ dependence is found. The relevance of this finding can be better appreciated in Fig. 4 (main panel) where we plot the $D(E_F)$ values together with the Curie temperature of each $Sr_{2-x}La_xFeMoO_6$ sample. A striking, almost linear, dependence of T_C on the $D(E_F)$ is obtained. This is a fundamental result that reveals and illustrates the role of the itinerant carriers on the ferromagnetic coupling in these oxides. The prediction that T_C may rise when increasing the $D(E_F)$ contained in the formalism of analysis of the effective moment and ferromagnetic coupling recently developed by Tovar *et al.*[10] was at the heart of the attempts to rise T_C by electron doping.[20] It is worth noting that the density of states projected on the Fe state, as determined from the PES obtained at $h\nu=90$ eV [open circles in Fig. 4 (inset)], does not show any significant variation upon La doping thus illustrating that doping carriers occupy mainly Mo orbitals.

The data shown here do not provide insight into the microscopic mechanism for the modification of the density of states, although it is clearly triggered by the La doping. The difficulty arises due to the fact that the carrier injection associated to the La doping is accompanied by a gradual cell expansion and structural distortion and the enhanced presence of antisites.[20] These effects are the result of the different sizes of La/Sr ions and a reduced driving force for Fe/Mo ordering due to the electron injection. The latter would be consistent with doping electrons occupying Mo-4*d* orbitals[21] and thus in agreement with the present data. The former may reduce the Mo-O-Fe orbital overlapping thus shrinking the conduction band. However, to what extent these phenomena contribute to the observed modifications of the $D(E_F)$ is nowadays unknown and further efforts to discriminate between bond bending, antisites and genuine carrier doping are required to address this issue.

IV. CONCLUSIONS

In summary, we have provide evidence that, in double perovskites, there is a close connection between the $D(E_F)$ and the strength of the ferromagnetic coupling and thus the Curie temperature. This experimental observation should provide a solid guide for research of half-metallic ferromagnetic oxides having still higher T_C and consequently opportunities for further developments of materials for spintronics. We shall mention that recent findings in ferromagnetic diluted semiconductors[27] also fit in the framework and methodologies developed here and thus the present results may have impact in areas of major current activity. On the other hand, Pickett[28] recently proposed that $A_2MM'O_6$ oxides could be ideal candidates for searching exotic spin-compensated half-metallic antiferromagnetism and eventually single spin superconductivity. Our observation that the spin-down carrier density can be adjusted by appropriate doping may provide an alternative way to reach the required fully spin compensation.

ACKNOWLEDGMENTS

We thank the AMORE (CEE), LURE, Project Nos. MAT 2002-04551-CO3-01 and MAT 2002-03431 for financial support and the MCYT-LURE for making available the synchrotron radiation light.

[1] K.-I. Kobayashi, T. Kimura, H. Sawada, K. Terakura, and Y. Tokura, Nature (London) **395**, 677 (1998).
[2] K.-I. Kobayashi, T. Kimura, Y. Tomioka, H. Sawada, K. Terakura, and Y Tokura, Phys. Rev. B **59**, 11 159 (1999).
[3] W.E. Pickett and D.J. Singh, Phys. Rev. B **53**, 1146 (1996), and references therein.
[4] H. Wu, Phys. Rev. B **64**, 125126 (2001).
[5] Ll. Balcells, J. Navarro, M. Bibes, A. Roig, B. Martínez, and J. Fontcuberta, Appl. Phys. Lett. **78**, 781 (2001); J.M. Greneche, M. Venkatesan, R. Suryanarayanan, and J.M.D. Coey, Phys. Rev. B **63**, 174403 (2001).
[6] D.D. Sarma, P. Mahadevan, T. Saha-Dasgupta, S. Ray, and A. Kumar, Phys. Rev. Lett. **85**, 2549 (2000); Z. Fang, K. Terakura, and J. Kanamori, Phys. Rev. B **63**, 180407(R) (2001).
[7] J.-S. Kang, H. Han, B.W. Lee, C.G. Olson, S.W. Han, K.H. Kim, J.I. Jeong, J.H. Park, and B.I. Min, Phys. Rev. B **64**, 024429 (2001).
[8] T. Saitoh, M. Nakatake, A. Kakizaki, H. Nakajima, O. Morimoto, Sh. Xu, Y. Moritomo, N. Hamada, and Y. Aiura, Phys. Rev. B **66**, 035112 (2002).
[9] S. Ray, A. Kumar, D.D. Sarma, R. Cimino, S. Turchini, S. Zennaro, and N. Zerma, Phys. Rev. Lett. **87**, 097204 (2001).
[10] M. Tovar, M.T. Causa, A. Butera, J. Navarro, B. Martínez, J. Fontcuberta, and M.C.G. Passeggi, Phys. Rev. B **66**, 024409 (2002).
[11] Z. Fang, K. Terakura, and J. Kanamori, Phys. Rev. B **63**, 180407(R) (2001).
[12] S. Nakayama, T. Nakagawa, and S. Nomura, J. Phys. Soc. Jpn. **24**, 219 (1968).
[13] Y. Moritomo, Sh. Xu, A. Machida, T. Akimito, E. Nishibori, M. Takata, and M. Sakata, Phys. Rev. B **61**, R7827 (2000).
[14] S. Nakagawa, J. Phys. Soc. Jpn. **24**, 806 (1968).
[15] M. Itoh, I. Ohta, and Y. Inaguma, Mater. Sci. Eng., B **B41**, 55 (1996).
[16] Y. Tomioka, T. Okuda, Y. Okimoto, R. Kumai, K.-I. Kobayashi, and Y. Tokura, Phys. Rev. B **61**, R7827 (2000).
[17] J. Lindén, T. Yamamoto, M. Karppinen, H. Yamauchi, and T. Pietari, Appl. Phys. Lett. **76**, 2925 (2000).
[18] O. Chmaissem, R. Kruk, B. Dabrowski, D.E. Brown, X. Xiong, S. Kolesnik, J.D. Jorgensen, and C.W. Kimball, Phys. Rev. B **62**, 14 197 (2000).
[19] B. Martínez, J. Navarro, Ll. Balcells, and J. Fontcuberta, J. Phys.: Condens. Matter **12**, 10 515 (2000).
[20] J. Navarro, C. Frontera, Ll. Balcells, B. Martínez, and J. Fontcuberta, Phys. Rev. B **64**, 092411 (2001).
[21] J.L. Alonso, L.A. Fernandez, F. Guinea, F. Lesmes, and V. Martin-Mayor, Phys. Rev. B **67**, 214423 (2003).
[22] Y. Huttel, F. Schiller, J. Avila, and M.C. Asensio, Phys. Rev. B **61**, 4948 (2000).
[23] M.E. Dávila, S.L. Molodtsov, M.C. Asensio, and C. Laubschat, Phys. Rev. B **62**, 1635 (2000).
[24] A. Arranz, J.F. Sánchez-Royo, J. Avila, V. Pérez-Dieste, P. Dumas, and M.C. Asensio, Phys. Rev. B **65**, 075405 (2002).
[25] S. Bengió, M. Martin, J. Avila, M.C. Asensio, and H. Ascolani, Phys. Rev. B **65**, 205326 (2002).
[26] C. Frontera *et al.*, Phys. Rev. B **68**, 012412 (2003).
[27] T. Dietl, H. Ohno, F. Matsukura, J. Cibert, and D. Ferrand, Science **287**, 1019 (2000), and references therein.
[28] W. Pickett, Phys. Rev. Lett. **77**, 3185 (1996).